Original Article

Formation of 7-carboxyheptyl radical induced by singlet oxygen in the reaction mixture of oleic acid, riboflavin and ferrous ion under the UVA irradiation

Hiroko Mori[1,2] and Hideo Iwahashi[1,*]

[1]Department of Chemistry, Wakayama Medical University, 580 Mikazura, Wakayama 641-8509, Japan
[2]Morinomiya College of Medical Arts and Sciences, 4-1-8 Nakamoto, Higashinariku, Osaka 537-0022, Japan

(Received 2 December, 2010; Accepted 21 February, 2011; Published online 13 July, 2011)

Identification of the radicals was performed for the standard reaction mixtures, which contained 4.3 mM oleic acid, 25 μM riboflavin, 1 mM $FeSO_4(NH_4)_2SO_4$, 10 mM cholic acid, 40 mM phosphate buffer (pH 7.4) and 0.1 M α-(4-pyridyl-1-oxide)-*N*-*tert*-butylnitrone under the UVA irradiation (365 nm), using an electron spin resonance, an high performance liquid chromatography-electron spin resonance and an high performance liquid chromatography-electron spin resonance-mass spectrometry. The electron spin resonance and high performance liquid chromatography-electron spin resonance measurements of the standard reaction mixtures showed prominent signals (α^N = 1.58 mT and $\alpha^H\beta$ = 0.26 mT) and peaks 1 and 3 (retention times, 37.0 min and 49.0 min). Since the peak 3 was not observed for the standard reaction mixture without oleic acid, the radical of the peak 3 seems to be derived from oleic acid. Singlet oxygens seem to participate in the formation of the oleic acid-derived radicals because the peak height of the peak 3 observed in the standard reaction mixture of D_2O increased to 308 ± 72% of the control. The high performance liquid chromatography-electron spin resonance-mass spectrometry analysis showed that 7-carboxyheptyl radical forms in the standard reaction mixture.

***Key Words*:** **oleic acid, lipid, radical, HPLC-ESR-MS, UVA**

Of the various oxidative stresses, UV irradiation is one of the primary factors. Chronic exposure of solar UV irradiations to mammalian skins induces a number of biological responses, including erythema, edema, sunburn cell formation, hyperplastic responses, photoaging and skin cancer development.[1–3] Increasing evidences showed that free radicals may be involved in the acute sunburn reactions.[4–6] Indeed, reactive oxygen speceis (ROS) such as hydrogen peroxide, $^1O_2$, $O_2^{-\bullet}$ and nitric oxide were detected under the UV irradiation.[7–11] Following UV-exposure, the ROS play a major role, in addition to DNA damage,[12] in producing lipid-derived radicals and the peroxidation of membrane lipids that seem to be responsible for the destruction of the cell membrane and ultimately the cell.[13–17] The UV-induced lipid peroxidation occurs either through a free radical chain reaction[14,15,17] or alternatively through a non-radical pathway by a direct reaction with singlet oxygen ($^1O_2$).[16,17]

Since UVB (315–280 nm) radiation constitutes only 5% of the solar UV radiation that reaches the surface of the earth, skin damages are not caused entirely by the UVB. Sufficient evidences indicated that UVA (400–315 nm) radiation, which accounts for the major portion of the solar UV radiation leads to skin damages.[18,19] The UVA-induced damages would be mediated by endogenous and/or exogenous photosensitizers. A particularly interesting photosensitizer is riboflavin (Rf), a member of the vitamin B_2 complex, which is a natural compound present in most living organisms.[20] The Rf can potentially act as a natural endogenous photosensitizer.[21,22] The usual mechanism of action of this sensitizer is rather complex. The Rf photodecomposes under aerobic UV or visible irradiation, in most of the cases with the concurrent involvement of ROS such as singlet oxygen ($^1O_2$) and superoxide anions ($O_2^{-\bullet}$).[20,23–26]

In spite of the intensive ESR studies on the reaction of Rf with natural or external compounds under the UVA irradiation, the radical species formed in the reaction mixtures have not been identified. In order to clarify the mechanism of UVA-induced skin damages mediated by endogenous and/or exogenous photosensitizers, in this study, identification of the lipid-derived radicals was performed for the standard reaction mixture which contained 4.3 mM oleic acid, 25 μM riboflavin, 1 mM $FeSO_4(NH_4)_2SO_4$, 10 mM cholic acid, 40 mM phosphate buffer (pH 7.4), and 0.1 M α-(4-pyridyl-1-oxide)-*N*-*tert*-butylnitrone under the UVA irradiation (365 nm) using the ESR, the HPLC-ESR and the HPLC-ESR-MS.[27] A spin trap reagent, α-(4-pyridyl-1-oxide)-*N*-*tert*-butylnitrone (4-POBN) was used to trap the lipid-derived radicals.

Materials and Methods

Chemicals. α-(4-Pyridyl-1-oxide)-*N*-*tert*-butylnitrone (4-POBN) was purchased from Tokyo Kasei Kogyo, Ltd. (Tokyo, Japan). Sodium azide and Rf were purchased from Wako Pure Chemical Industries (Osaka, Japan). Superoxide dismutase (SOD) from bovine erythrocytes and catalase from bovine liver were from Sigma-Aldrich Co. (St. Louise, MO). All other chemicals used were of analytical grade.

ESR studies. The ESR experiments were carried out on a JES-FR 30 Free Radical Monitor (JEOL Ltd., Tokyo, Japan). Operating conditions of the ESR spectrometer were: power, 4 mW; modulation width, 0.1 mT; time constant, 0.3 sec. Magnetic fields were calculated by the splitting of MnO (ΔH_{3-4} = 8.69 mT).

HPLC-ESR chromatography. An HPLC used in the HPLC-ESR consisted of a model 7125 injector (Reodyne, Cotati, CA), a model L-7100 pump (Hitachi Ltd., Ibaragi, Japan). A semi-preparative column (300 mm long × 10 mm i.d.) packed with TSKgel ODS-120T (TOSOH Co., Tokyo, Japan) was used. Flow

*To whom correspondence should be addressed.
E-mail: chem1@wakayama-med.ac.jp

doi: 10.3164/jcbn.10-144

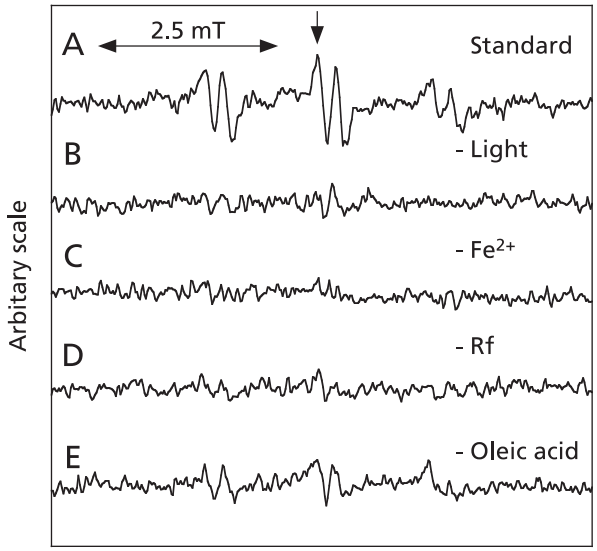

Fig. 1. ESR spectra of the standard reaction mixtures of oleic acid, Rf and ferrous ions under the UVA irradiation. The reaction and ESR conditions were as described in Materials and Methods. (A) An ESR spectrum of the standard reaction mixture. (B) An ESR spectrum of the standard reaction mixture without light. (C) An ESR spectrum of the standard reaction mixture without Fe^{2+}. (D) An ESR spectrum of the standard reaction mixture without Rf. (E) An ESR spectrum of the standard reaction mixture without oleic acid.

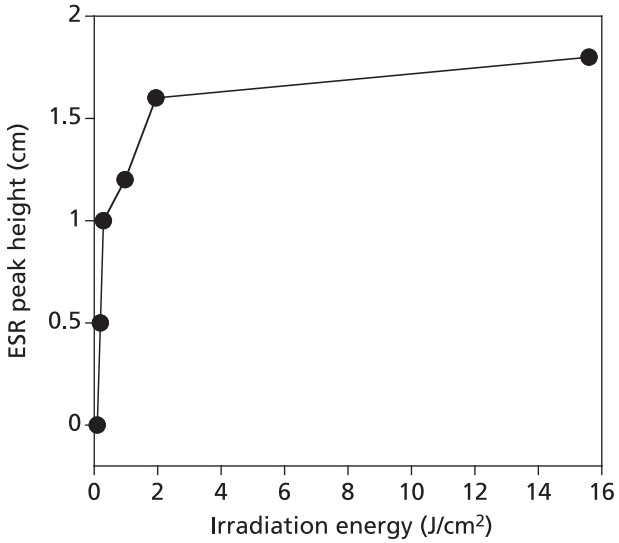

Fig. 2. Irradiation energy dependence of the ESR peak heights. The reaction and ESR conditions were as described in Materials and Methods except for the irradiation energies.

rate was 2.0 ml/min throughout the HPLC-ESR experiments. For the HPLC-ESR, two solvents were used: solvent A, 50 mM acetic acid; solvent B, 50 mM acetic acid/acetonitrile (20:80, v/v). A following combination of isocratic and linear gradient was used: 0–40 min, 100% A to 20% A (linear gradient); 40–75 min, 80% B (isocratic). The eluent was introduced into a model JES-FR30 Free Radical Monitor (JEOL Ltd., Tokyo, Japan). The ESR spectrometer was connected to the HPLC with a Teflon tube, which passed through the center of the ESR cavity. The operating conditions of the ESR spectrometer were: power, 4 mW; modulation width, 0.2 mT; time constant, 1 sec. The magnetic field was fixed at the third peak in the double-triplet ESR spectrum (α^N = 1.58 mT and $\alpha^H\beta$ = 0.26 mT) of the 4-POBN radical adducts (Fig. 1).

HPLC-ESR-MS chromatography. The HPLC and ESR conditions were as described in the HPLC-ESR. The mass spectrometer (MS) used in the HPLC-ESR-MS was a model M-1200 HS electrospray ionization (ESI)-MS (Hitachi Ltd., Ibaragi, Japan). The operating conditions of the ESI-MS were: nebulizer, 180°C; aperture1, 120°C; N_2 controller pressure, 19.6 N/cm^2; drift voltage, 70 V; multiplier, 2000 V; needle voltage, 4000 V; polarity, positive; resolution, 48. The mass spectra were obtained by introducing the eluent from the ESR detector into the ESI-MS system just before the peak was eluted. The flow kept at 50 μl/min while the eluent was introducing into the ESI-MS.

Standard reaction conditions. The standard reaction mixture contained 4.3 mM oleic acid, 25 μM Rf, 40 mM phosphate buffer (pH 7.4), 10 mM cholic acid, 0.1 M 4-POBN and 1 mM $FeSO_4(NH_4)_2SO_4$ in a quartz test tube (100 mm long × 8 mm i.d.). The standard reaction mixtures without 1 mM $FeSO_4(NH_4)_2SO_4$ and 0.1 M 4-POBN were exposed to 7.8 J/cm^2 UVA light under air using a 400 W UV lamp and a LXO365 bandpass filter (365 nm) (ASAHI SPECTRA Co., Tokyo, Japan). After the UVA irradiation, 0.1 M 4-POBN was added. The reactions were started by adding 1 mM $FeSO_4(NH_4)_2SO_4$ and performed at 25°C for 1 min. The reaction mixtures were aspirated into a Teflon tube centered in an ESR microwave cavity. And then, ESR spectra were measured.

Reaction in D_2O. After water was removed from the standard reaction mixture without 0.1 M 4-POBN and 1 mM $FeSO_4(NH_4)_2SO_4$ using centrifugal concentrator cc-105 (Tomy Seiko Co., Ltd., Tokyo, Japan), D_2O was added to the reaction mixture. The other reaction conditions were as described for the standard reaction conditions. The control reaction was performed by addition of H_2O instead of D_2O.

Results

ESR measurements of the standard reaction mixtures under the UVA irradiation. ESR spectra were measured for the standard reaction mixtures under the UVA irradiation (Fig. 1). A prominent ESR spectrum (α^N = 1.58 mT and $\alpha^H\beta$ = 0.26 mT) was observed in the standard reaction mixture (Fig. 1A), suggesting that free radicals form in the standard reaction mixture. The ESR spectrum was hardly observed for the standard reaction mixture without the UVA irradiation (or Fe^{2+}, or Rf, or oleic acid) (Figs. 1 B–E).

UVA irradiation energy dependence of the ESR peak height. UVA irradiation energy dependence of the ESR peak height was observed (Fig. 2). The ESR peak height increased with increase of the irradiation energy, and reached a plateau at 2 J/cm^2.

HPLC-ESR analyses of the standard reaction mixtures under the UVA irradiation. To know which radicals formed in the standard reaction mixtures of oleic acid, Rf and iron ions under the UVA irradiation, the HPLC-ESR analyses were performed for the standard reaction mixtures at a modulation of 0.2 mT. Prominent peaks (peaks 1 and 3) were observed on the HPLC-ESR elution profile of the standard reaction mixture under the UVA irradiation (Fig. 3A). The retention times of the peaks 1 and 3 are 37.0 and 49.0 min, respectively. The peak 3 was hardly observed for the standard reaction mixture without the UVA irradiation (or Fe^{2+}, or Rf, or oleic acid) (Figs. 3 B–E). The peak 1 was not observed for the standard reaction mixture without Rf (Fig. 3D).

HPLC-ESR-MS analyses of the standard reaction mixtures under the UVA irradiation. To determine the structures of the peak 1 and peak 3 compounds observed on the HPLC-ESR elution profile of the standard reaction mixture under the UVA irradiation, the HPLC-ESR-MS analyses were performed at a modulation of

doi: 10.3164/jcbn.10-144

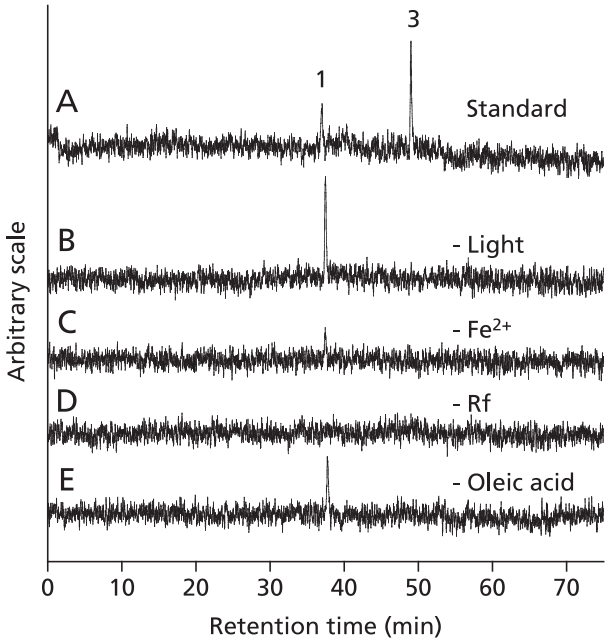

Fig. 3. HPLC-ESR analyses of the standard reaction mixtures. The reaction and HPLC-ESR conditions were as described in Materials and Methods. (A) The standard reaction mixture. (B) The standard reaction mixture without light. (C) The standard reaction mixture without Fe^{2+}. (D) The standard reaction mixture without Rf. (E) The standard reaction mixture without oleic acid.

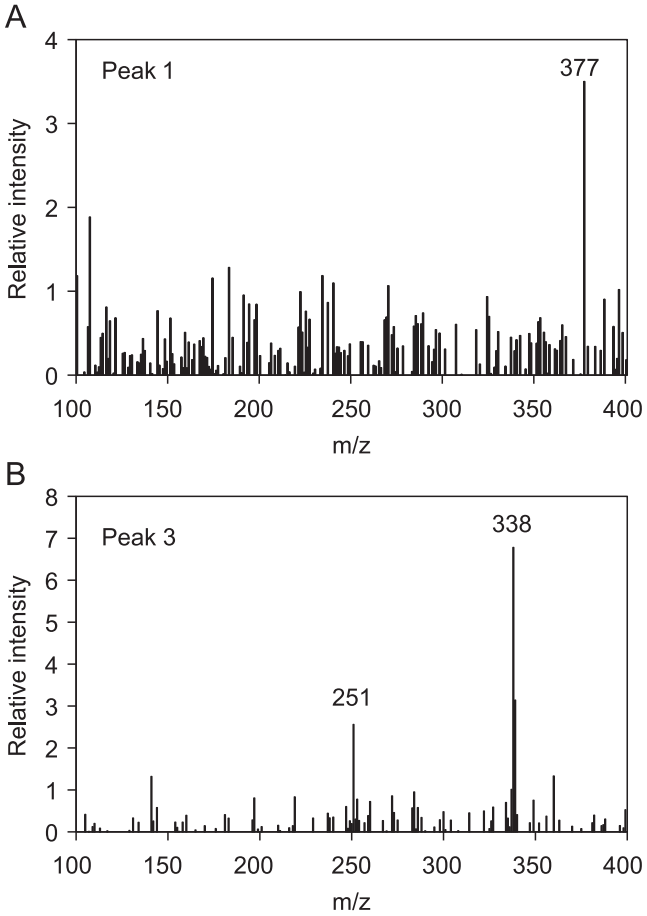

Fig. 4. HPLC-ESR-MS analyses of the peaks 1 and 3. The reaction and HPLC-ESR-MS conditions were as described in Materials and Methods. (A) Peak 1. (B) Peak 3.

0.2 mT. The HPLC-ESR-MS analysis of the peak 1 compound gave ions at m/z 377 (Fig. 4A). The ions at m/z 377 correspond to the protonated molecules of Rf, $[M + H]^+$. ESR spectra of the peak 1 were measured (Fig. 5). Although no ESR signal was observed at a modulation of 0.1 mT (Fig. 5A), a broad ESR signal was observed at a modulation of 0.2 mT (Fig. 5B), suggesting that a relatively stable Rf radical with broad ESR signals forms in the reaction mixture.

The HPLC-ESR-MS analysis of the peak 3 compound gave ions at m/z 251 and m/z 338 (Fig. 4B). The ions at m/z 338 correspond to the protonated molecules of the 4-POBN/7-carboxyheptyl radical adducts, $[M + H]^+$. The fragment ions at m/z 251 correspond to the loss of $(CH_3)_3C(O)N$ from the protonated molecules.

Effects of some compounds on the ESR and HPLC-ESR peak heights. To know whether singlet oxygens are involved in the radical formation, the reactions were performed in D_2O. The ESR peak heights which were observed for the reaction in D_2O increased to 248 ± 9% of the control (Table 1). The HPLC-ESR peak height of the peak 3 which were observed for the reaction in D_2O also increased to 308 ± 72% of the control.

When a singlet oxygen scavenger, azide was added to the standard reaction mixtures of oleic acid, the ESR peak height interestingly increased to 198 ± 14% (156 ± 26%) of the control under the 7.8 J/cm^2 (1.95 J/cm^2) UVA irradiation (Table 1). To check the pH change due to the addition of 20 mM sodium azide, the reactions were performed in the 140 mM phosphate buffer (pH 7.4). On addition of 20 mM sodium azide, the ESR peak height of the oleic acid-derived radicals also increased to 149 ± 3% of the control even in the 140 mM phosphate buffer under the 1.95 J/cm^2 UVA irradiation (Table 1). On addition of 0.2 mM sodium azide, the ESR peak height also increased to 157 ± 27% of the control under the 1.95 J/cm^2 UVA irradiation (Table 1). Thus, sodium azide seems to enhance the radical formation under various conditions. To investigate which radicals form in the standard reaction mixture with sodium azide, HPLC-ESR and HPLC-ESR-

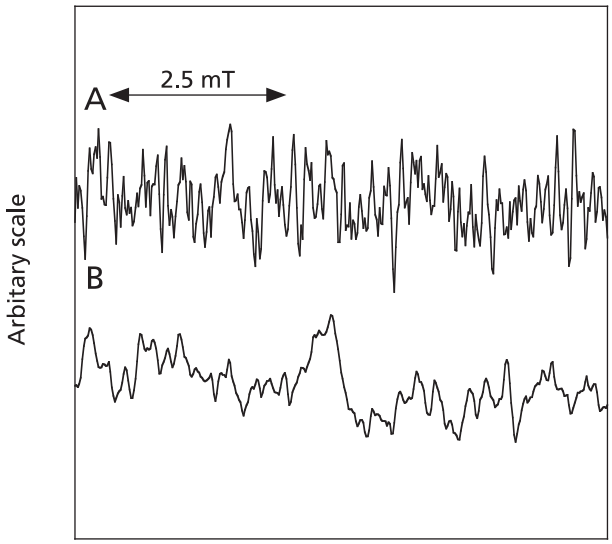

Fig. 5. ESR spectra of the peak 1. The reaction, ESR and HPLC-ESR conditions were as described in Materials and Methods except for the modulation values. (A) 0.1 mT. (B) 0.2 mT.

Table 1. Effects of some compounds on the ESR peak heights (ESR) and peak 3 peak heights (HPLC-ESR)

compounds added and irradiation energies	% control
D_2O (ESR), 7.8 J/cm^2	248 ± 9
D_2O (HPLC-ESR), 7.8 J/cm^2	308 ± 72
Azide (20 mM)(ESR), 7.8 J/cm^2	198 ± 14
Azide (20 mM)(ESR), 1.95 J/cm^2	156 ± 26
Azide (20 mM)(ESR), 1.95 J/cm^2	149 ± 3*
Azide (0.2 mM)(ESR), 1.95 J/cm^2	157 ± 27
SOD (300 units/ml)(ESR), 1.95 J/cm^2	95 ± 5.5
Catalase (1260 units/ml)(ESR), 1.95 J/cm^2	115 ± 23

Results are means ± SD of three experiments. The reactions were performed as described in Materials and Methods excect for the data indicated by *. The data indicated by * were obtained under the same conditons as Materials and Methods except for the concentration of phosphate buffer. The concentration of phosphate buffer was 140 mM.

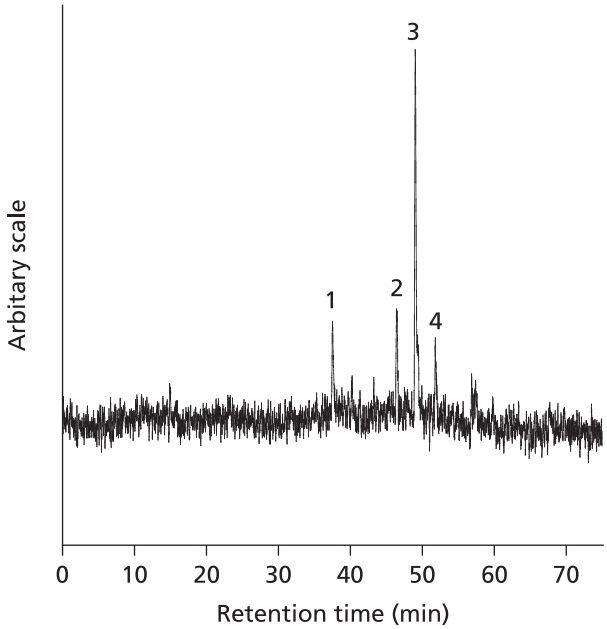

Fig. 6. The HPLC-ESR analysis of the standard reaction mixture with 20 mM sodium azide. The reaction and HPLC-ESR conditions were as described in Materials and Methods except for the total volume and the composition of the reaction mixture. The total volume of the reaction mixture was 3.0 ml. The standard reaction mixture with 20 mM sodium azide was analyzed using the HPLC-ESR.

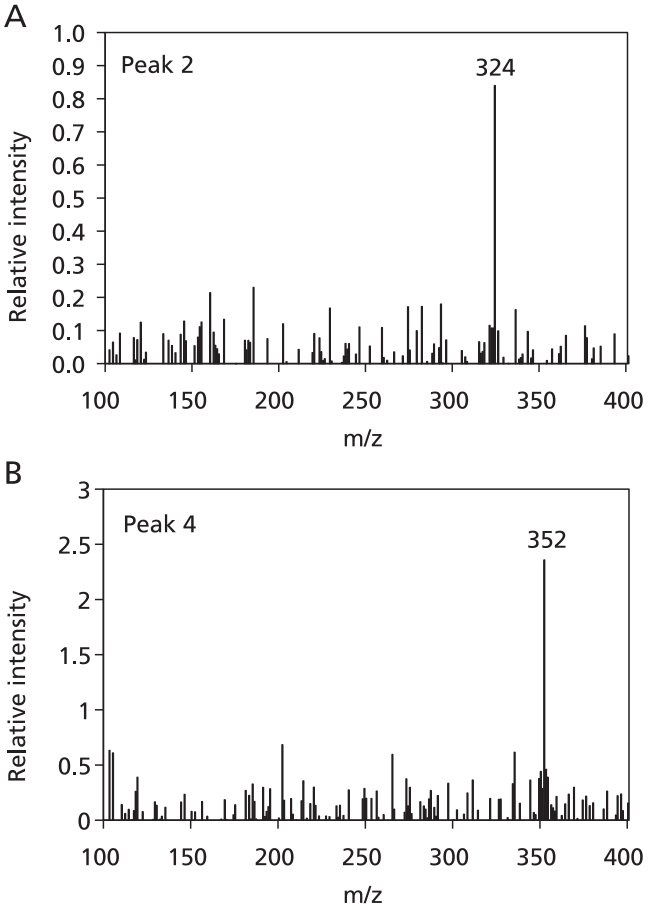

Fig. 7. HPLC-ESR-MS analyses of the peaks 2 and 4 observed for the standard reaction mixture with sodium azide. The reaction and HPLC-ESR-MS conditions were as described in Materials and Methods except for the total volume and the composition of the reaction mixture. The total volume of the reaction mixture was 3.0 ml. The standard reaction mixture with 20 mM sodium azide was analyzed using the HPLC-ESR-MS. (A) Peak 2. (B) Peak 4.

MS analyses were performed (Figs. 6 and 7). The HPLC-ESR analysis detected four peaks (peaks 1–4) at the retention times of 37.6 min, 46.5 min, 49.0 min and 51.8 min. Based on the retention times, the peaks 1 and 3 correspond to Rf radicals and 4-POBN/7-carboxyheptyl radical adducts, $[M + H]^+$. The HPLC-ESR-MS analyses of the two new peaks (peaks 2 and 4) were performed (Fig. 7). The HPLC-ESR-MS analysis of the peak 2 compound gave ions at m/z 324 (Fig. 7A). The ions at m/z 324 correspond to the protonated molecules of the 4-POBN/6-carboxyhexyl radical adducts, $[M + H]^+$. The HPLC-ESR-MS analysis of the peak 4 compound gave ions at m/z 352 (Fig. 7B).

To investigate the effect of SOD on the radical formation, the ESR measurements were performed for the standard reaction mixtures with SOD (Table 1). On addition of 300 units/ml SOD under the 1.95 J/cm^2 UVA irradiation, the ESR peak height kept unchanged (Table 1).

To know whether or not hydrogen peroxide is involved in the radical formation, the effect of catalase was examined. When 1260 units/ml catalase was added to the standard reaction mixtures under the 1.95 J/cm^2 UVA irradiation, no change was observed in the ESR peak height (Table 1).

Discussion

In the present investigation, it was shown that the 7-carboxyheptyl radical form in the standard reaction mixture under the UVA irradiation. SOD and catalase exerted little effect on the radical formation. Superoxide anions and hydrogen peroxide do not mainly participate in the formation of the oleic acid-derived radicals. When the reaction was performed in D_2O, the ESR peak height increased. Thus, singlet oxygens seem to be involved in the formation of the oleic acid-derived radicals because D_2O increases the lifetime of singlet oxygens.[28]

A possible reaction path for the formation of the 7-carboxyheptyl radical is as follows (Fig. 8). The excited singlet state sensitizer ^{1}(Riboflavin)*, which is produced under the UVA irradiation turns to the excited triplet state ^{3}(Riboflavin)* through intersystem crossing. The excited triplet state ^{3}(Riboflavin)* may reacts with triplet oxygen to form singlet oxygen (Eq. 1).[26,29]

doi: 10.3164/jcbn.10-144

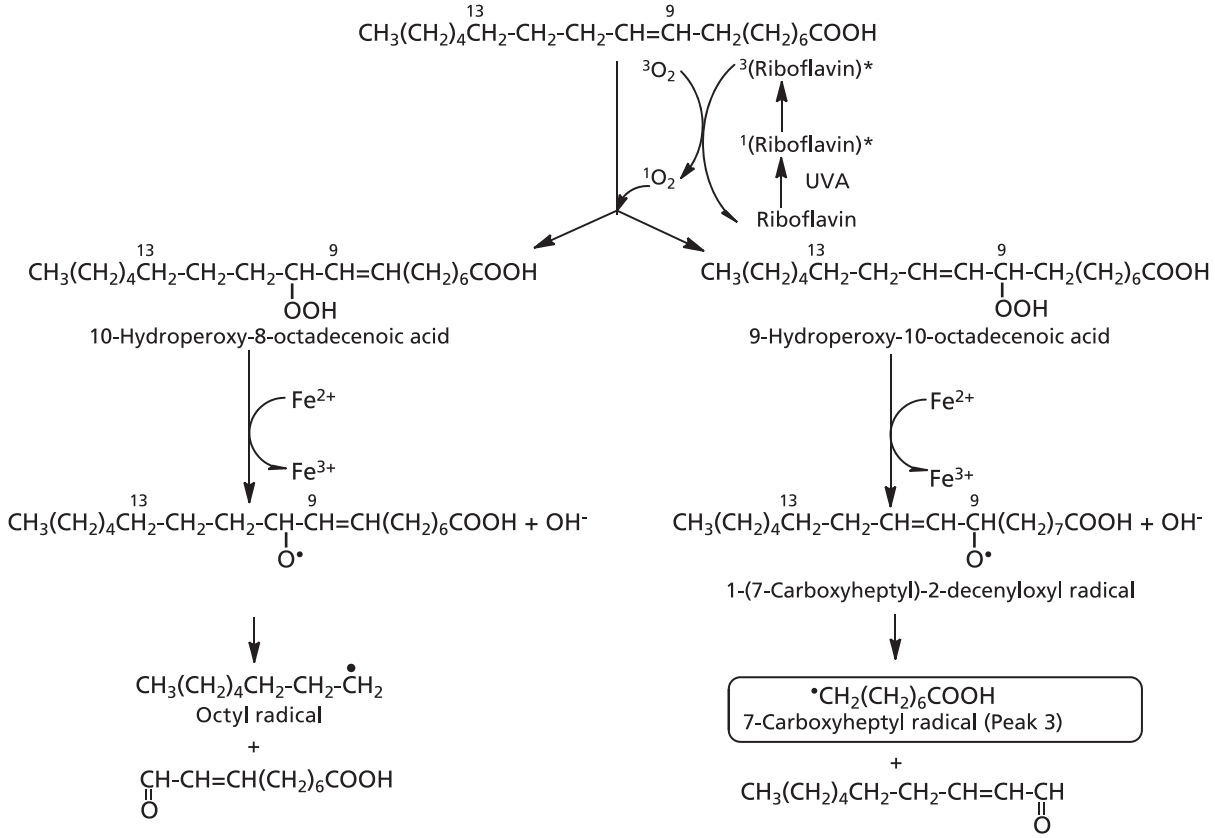

Fig. 8. A possible reaction path for the formation of the 7-carboxyheptyl radical (Peak 3) in the standard reaction mixture.

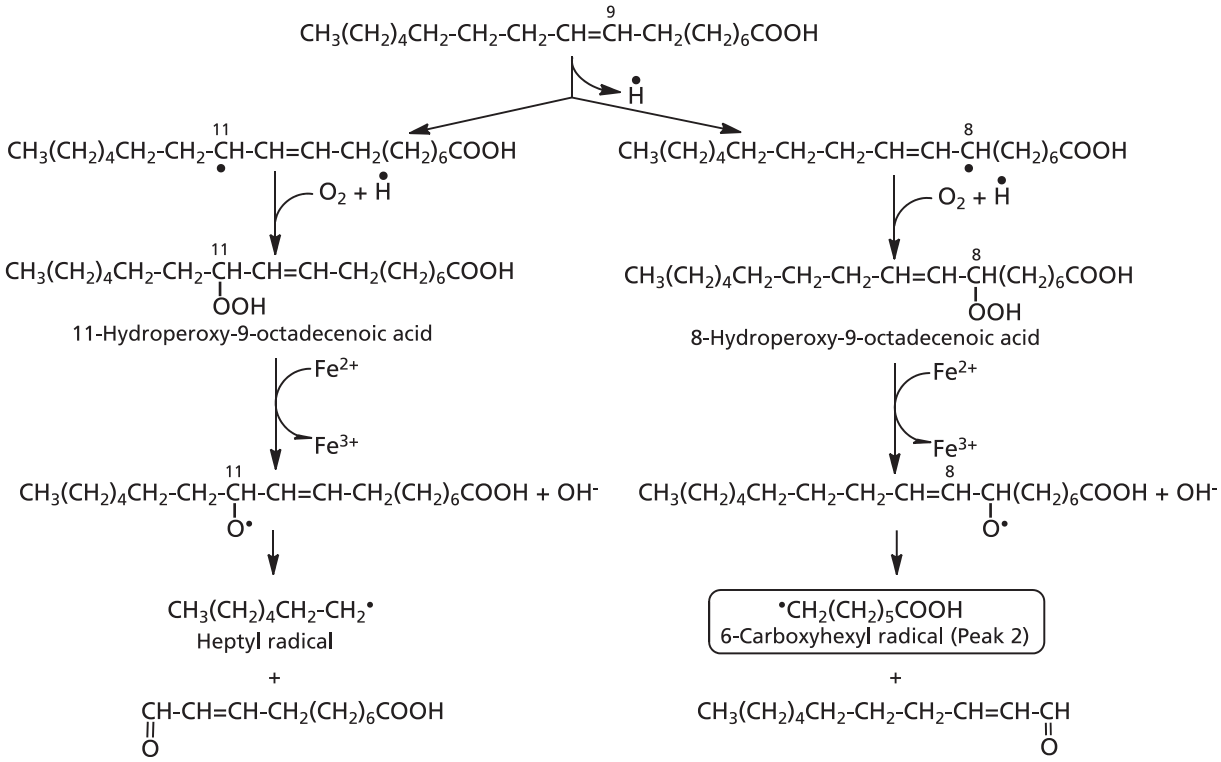

Fig. 9. A possible reaction path for the formation of the 6-carboxyhexyl radical (Peak 2) in the standard reaction mixture with sodium azide.

^{3}(Riboflavin)* + $^3O_2$ → Riboflavin + $^1O_2$.....(1)

The reaction of oleic acid with the singlet oxygen results in the formation of LOOH (9-hydroperoxy-10-octadecenoic acid or 10-hydroperoxy-8-octadecenoic acid) through the singlet oxygen ene reaction (Eq. 2).[30]

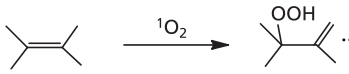

.....(2)

Ferrous ions possibly catalyze decomposition of the 9-hydroperoxy-10-octadecenoic acid. This reaction yields a radical intermediate LO•[1-(7-carboxyheptyl)-2-decenyloxyl radical]. The β-scission of the LO• results in the generation of the 7-carboxyheptyl radical. The reaction of ferrous ion with the 10-hydroperoxy-8-octadecenoic acid would result in the formation of octyl radical. We could not detect the radical. Since the 4-POBN used in this experiment is a relatively polar molecule, octyl radical which is located at the non-polar area may be difficult to be trapped by the 4-POBN.

Addition of azide to the standard reaction mixture interestingly resulted in the increase of the ESR peak height and appearance of the two new peaks (peak 2 and 4) on the elution profile of the HPLC-ESR analysis. On addition of the singlet oxygen scavenger, azide, a reactive compound which can subtract hydrogen atoms from oleic acid or Rf may form in the reaction mixture. The H-abstraction of oleic acid at C8 result in the formation of 8-hydroperoxy-9-octadecenoic acid (Fig. 9). Ferrous ions possibly catalyze decomposition of the 8-hydroperoxy-9-octadecenoic acid. This reaction yields a radical intermediate LO•[1-(6-carboxyhexyl)-2-undecenyloxyl radical]. The β-scission of the LO• could result in the generation of the 6-carboxyhexyl radical (Fig. 6, peak 2). On the other hand, The H-abstraction of oleic acid at C11 could result in the formation of heptyl radical. We could not detect the radical. Since the 4-POBN used in this experiment is a relatively polar molecule, heptyl radical which is located at the non-polar area may be difficult to be trapped by the 4-POBN. The H-abstraction of Rf could result in the formation of Rf radical.

References

1 Mukhtar H, Elmets CA. Photocarcinogenesis: mechanisms, models and human health implications. *Photochem Photobiol* 1996; **63**: 356–357.
2 Goihman-Yahr M. Skin aging and photoaging: An outlook. *Clin Dermatol* 1996; **14**: 153–160.
3 Young AR. Cumulative effects of ultraviolet radiation on the skin: cancer and photoaging. *Semin Dermatol* 1990; **9**: 25–31.
4 Taira J, Mimura K, Yoneya T, Hagi A, Murakami A, Makino K. Hydroxyl radical formation by UV-irradiated epidermal cells. *J Biochem* 1992; **111**: 693–695.
5 Jurkiewicz BA, Buettner GR. Ultraviolet light-induced free radical formation in skin: an electron paramagnetic resonance study. *Photochem Photobiol* 1994; **59**: 1–4.
6 Shindo Y, Witt E, Han D, Packer L. Dose-response effects of acute ultraviolet irradiation on antioxidants and molecular markers of oxidation in murine epidermis and dermis. *J Invest Dermatol* 1994; **102**: 470–475.
7 Katiyar SK, Afag F, Perez A, Mukhtar H. Green tea polyphenol (–)-epigallocatechin-3-gallate treatment of human skin inhibits ultraviolet radiation-induced oxidative stress. *Carcinogenesis* 2001; **22**: 287–294.
8 Pathak MA, Joshi PC. Production of active oxygen species ($^1O_2$ and $O_2^{\cdot-}$) by psoralens and ultraviolet radiation (320–400 nm). *Biochim Biophys Acta* 1984; **798**: 115–126.
9 Herring T, Fuchs J, Rehberg J, Groth N. UV-induced free radicals in the skin detected by ESR spectroscopy and imaging using nitroxides. *Free Radic Biol Med* 2003; **35**: 59–67.
10 Herrling T, Jung K, Fuchs J. Measurements of UV-generated free radicals/reactive oxygen species (ROS) in skin. *Spectrochim Acta A Mol Biomol Spectrosc* 2006; **63**: 840–845.
11 Haywood R, Rogge F, Lee M. Protein, lipid, and DNA radicals to measures skin UVA damage and modulation by melanin. *Free Radic Biol Med* 2008; **44**: 990–1000.
12 Tanaka M, Ohkubo K, Fukuzumi S. DNA cleavage by UVA irradiation of NADH with dioxygen via radical chain processes. *J Phys Chem A* 2006; **110**: 11214–11218.
13 Ananthaswamy HN, Pierceall WE. Molecular mechanisms of ultraviolet radiation carcinogenesis. *Photochem Photobiol* 1990; **52**: 1119–1136.
14 Ogura R, Sugiyama M, Nishi J, Haramaki N. Mechanism of lipid radical formation following exposure of epidermal homogenate to ultraviolet light. *J Invest Dermatol* 1991; **97**: 1044–1047.
15 Mazari A, Iwamoto S, Yamauchi R. Ultraviolet A-induced peroxidation of phosphatidylcholine in unilamellar liposomes. *Biosci Biothechnol Biochem* 2009; **73**: 1212–1214.
16 Baier J, Maisch T, Regensburger J, Pöllmann C, Bäumler W. Optical detection of singlet oxygen produced by fatty acids and phospholipids under ultraviolet A irradiation. *J Biomed Opt* 2008; **13**: 044029-1-7.
17 Xia Q, Yin JJ, Cherng SH, *et al*. UVA photoirradiation of retinyl palmitate—formation of singlet oxygen and superoxide, and their role in induction of lipid peroxidation. *Toxicol Lett* 2006; **163**: 30–43.
18 Moan J, Dahlback A, Setlow RB. Epidemiological support for an hypothesis for melanoma induction indicating a role for UVA radiation. *Photochem Photobiol* 1999; **70**: 243–247.
19 Garland CF, Garland FC, Gorham ED. Epidemiologic evidence for different roles of ultraviolet A and B radiation in melanoma mortality rates. *Ann Epidemiol* 2003; **13**: 395–404.
20 Heelis PF. The photophysical and photochemical properties of flavins (isoalloxazines). *Chem Soc Rev* 1982; **11**: 15–39.
21 Edwards AM, Silva E. Effect of visible light on selected enzymes, vitamins and amino acids. *J Photochem Pohotobiol B* 2001; **63**: 126–131.
22 Massad WA, Barbieri Y, Romero M, García NA. Vitamin B_2-sensitized photo-oxidation of dopamine. *Photochem Photobiol* 2008; **84**: 1201–1208.
23 Chacon JN, McLearie J, Sinclair RS. Singlet oxygen yields and radical contributions in the dye-sensitised photo-oxidation in methanol of esters of polyunsatured fatty acids (oleic, linoleic, linolenic and arachidonic). *Photochem Photobiol* 1988; **47**: 647–656.
24 Pajares A, Gianotti J, Stettler G, *et al*. Modelling the natural photodegradation of water contaminants: a kinetic study on the light-induced aerobic interactions between riboflavin and 4-hydroxypyridine. *Photochem Photobiol A* 2001; **139**: 199–204.
25 Ahmad I, Fasihullah Q, Noor A, Ansari IA, Ali QN. Photolysis of riboflavin in aqueous solution: a kinetic study. *Int J Pharm* 2004; **280**: 199–208.
26 Krishna CM, Uppuluri S, Riesz P, Zialer JS Jr., Balasubramanian D. A study of the photodynamic efficiencies of some eye lens constituents. *Photochem Photobiol* 1991; **54**: 51–58.
27 Iwahashi H. High performance liquid chromatography/electron spin resonance/mass spectrometry analyses of lipid-derived radicals. *Methods Mol Biol* 2008; **477**: 65–73.
28 Ameta SC, Punjabi PB, Chobisa CS, *et al*. Singlet molecular oxygen. *Asian J Chem Rev* 1990; **1**: 106–124.
29 Baier J, Maisch T, Maier M, Engel E, Landthaler M, Bäumler W. Singlet oxygen generation by UVA light exposure of endogeneous photosensitizers. *Biophys J* 2006; **91**: 1452–1459.
30 Stephenson LM. The mechanism of the singlet oxygen ene reaction. *Tetrahedron Lett* 1980; **21**: 1005–1008.

doi: 10.3164/jcbn.10-144